

# Narrowly avoided spin-nematic phase in BaCdVO(PO<sub>4</sub>)<sub>2</sub>: NMR evidence

K. M. Ranjith,<sup>1,2</sup> K. Yu. Povarov,<sup>3,4</sup> Z. Yan,<sup>3</sup> A. Zheludev,<sup>3,\*</sup> and M. Horvatić<sup>1,†</sup>

<sup>1</sup>Laboratoire National des Champs Magnétiques Intenses, LNCMI-CNRS (UPR3228), EMFL, Université Grenoble Alpes, UPS and INSA Toulouse, Boîte Postale 166, 38042 Grenoble Cedex 9, France

<sup>2</sup>Present address: IFW Dresden, Helmholtzstraße 20, 01069 Dresden, Germany

<sup>3</sup>Laboratory for Solid State Physics, ETH Zürich, 8093 Zürich, Switzerland

<sup>4</sup>Present address: Dresden High Magnetic Field Laboratory (HLD-EMFL) and Würzburg-Dresden Cluster of Excellence *ct.qmat*, Helmholtz-Zentrum Dresden-Rossendorf, 01328 Dresden, Germany

(Dated: January 11, 2024)

We present a <sup>31</sup>P nuclear magnetic resonance (NMR) investigation of BaCdVO(PO<sub>4</sub>)<sub>2</sub> focusing on the nearly saturated regime between  $\mu_0 H_{c1} = 4.05$  T and  $\mu_0 H_{c2} = 6.5$  T, used to be considered as a promising candidate for a spin-nematic phase. NMR spectra establish the absence of any dipolar order there, whereas the weak field dependence of the magnetization above  $H_{c1}$  is accounted for by Dzyaloshinskii-Moriya interaction terms. The low-energy spin dynamics (fluctuations), measured by nuclear spin-lattice relaxation rate ( $T_1^{-1}$ ), confirms the continuity of this phase and the absence of any low-temperature phase transition. Unexpectedly, the spin dynamics above  $H_{c1}$  is largely dominated by two-magnon processes, which is expected *above* the saturation field of a spin-nematic phase, but not inside. This shows that BaCdVO(PO<sub>4</sub>)<sub>2</sub> is indeed close to a spin-nematic instability, however, this phase is *not* stabilized. We thus confirm recent theoretical predictions that the spin-nematic phase can be stabilized, at most, in an extremely narrow field range close to saturation or is rather narrowly avoided [Jiang *et al.*, Phys. Rev. Lett. **130**, 116701 (2023)].

## INTRODUCTION

One good place to look for exotic quantum phases in magnetic insulators is in frustrated antiferromagnets (AFs) close to a classical ferromagnetic (FM) instability [1, 2]. On very general arguments, in the applied magnetic field these systems either enter saturation in a (weakly) discontinuous transition or exhibit some kind of purely quantum “pre-saturation phase”. One of the most famous examples is  $S = 1/2$  Heisenberg square-lattice model with FM nearest-neighbor (nn) coupling  $J_1$  and frustrating AF next nearest neighbor (nnn) interaction  $J_2$ . Near saturation, it has been predicted to support the so-called spin-nematic state [1, 3, 4] for a wide range of frustration ratio  $J_2/J_1$ . The simple physical picture is condensation of bound magnon pairs stabilized by the ferromagnetic bonds. The energy of such pairs is lower than that of two free magnons. Thus, upon lowering the field in the fully polarized state, they condense before the conventional one-magnon BEC, responsible for Néel (dipolar) order, can take place.

To date, this type of multipolar ordered phase remained experimentally as elusive as quantum spin liquids. The materials that most closely correspond to this model are the quasi-two-dimensional (quasi-2D) layered vanadyl phosphates with the general formula  $AA'VO(PO_4)_2$  ( $A, A' = Ba, Cd, Pb, Sr, Zn$ ) [5–7]. In at least two species,  $Pb_2VO(PO_4)_2$  and  $SrZnVO(PO_4)_2$ , rather unusual narrow pre-saturation phases have been discovered, but shown to represent some kind of complex dipolar-ordered, rather than nematic states [8–11].

Of all these compounds the most frustrated and the most promising spin-nematic candidate is

BaCdVO(PO<sub>4</sub>)<sub>2</sub> [6, 7]. Indeed, recent studies have produced thermodynamic and neutron diffraction evidence that this material may have a novel exotic quantum phase in applied fields above  $\mu_0 H_{c1} = 4.0$  T where Neel order disappears [12, 13]. Even though the spin Hamiltonian of BaCdVO(PO<sub>4</sub>)<sub>2</sub> is by now very well characterized [14], the origin of this high-field phase remains unclear. In particular, it persists in magnetic field all the way up to  $H_{c2} = 6.5$  T. Such a wide field range is difficult to reconcile even with predictions based on the simplistic magnon-pair mechanism [1, 3]. Most recent theoretical studies take magnon-pair interactions into account and conclude that stability range for the spin-nematic phase must be lower by yet another order of magnitude [15]. Another concern are the subtle but relevant magnetic anisotropies in different  $AA'VO(PO_4)_2$  crystal structures, such as complex Dzyaloshinskii-Moriya (DM) interactions and patterns of  $g$ -tensor canting.

Here, we report the results of an NMR study aimed at better understanding the saturation process. We show that, unlike the pre-saturation phases  $Pb_2VO(PO_4)_2$  and  $SrZnVO(PO_4)_2$ , the high-field phase in BaCdVO(PO<sub>4</sub>)<sub>2</sub> has no dipolar order of any kind. At the same time, measurements of NMR relaxation rates independently confirm the high-field continuous phase transition at  $H_{c2}$ . Finally, we show that the in-between phase is characterized by very unusual spin relaxation that is dominated by two-magnon processes.

## MATERIAL AND EXPERIMENTAL DETAILS

The crystal structure and geometry of magnetic interactions in  $\text{BaCdVO}(\text{PO}_4)_2$  is discussed in detail elsewhere [14]. Here we only recall that at room temperature the space group is orthorhombic,  $P_{bca}$ , with lattice parameters  $a = 8.84 \text{ \AA}$ ,  $b = 8.92 \text{ \AA}$ , and  $c = 19.37 \text{ \AA}$ . There are  $2 \times 4 = 8$  magnetic  $S = 1/2 \text{ V}^{4+}$  ions per cell, arranged in proximate square lattice layers in the  $(a, b)$  plane, two layers per cell. The symmetry is further lowered to  $P_{ca}21$  in a structural transition at  $T_s \sim 240 \text{ K}$ , resulting in 8 distinct nn and nnn superexchange paths within each layer. Magnetic order sets in at  $T_N \approx 1.05 \text{ K}$  and is of a “up-up-down-down” character [16], naturally following the alternation of nn interaction strengths along the crystallographic  $a$  axis [12].

NMR experiments were performed on a green transparent single crystal sample ( $3.2 \times 2.5 \times 0.35 \text{ mm}^3$ ) from the same batch as those studied in Refs. [12–14]. The sample was oriented to have the  $c$  axis parallel to the applied magnetic field  $\mathbf{H}$ , and was placed inside the mixing chamber of a  $^3\text{He}$ - $^4\text{He}$  dilution refrigerator for the measurements below 1 K, or in the standard cold-bore variable temperature insert (VTI) for temperatures  $\geq 1.4 \text{ K}$ .

The  $^{31}\text{P}$  NMR spectra were taken by standard spin-echo sequence and the frequency-sweep method. The nuclear spin-lattice relaxation rate  $T_1^{-1}$  was measured by the saturation-recovery method and the time ( $t$ ) recovery of the nuclear magnetization  $M(t)$  after a saturation pulse was fitted by the stretched exponential function,  $M(t)/M_0 = 1 - C \exp[-(t/T_1)^{\beta_s}]$ , where  $M_0$  is the equilibrium nuclear magnetization,  $C \cong 1$  accounts for the imperfection of the excitation (saturation) pulse, and  $\beta_s$  is the stretching exponent to account for possible inhomogeneous distribution of  $T_1^{-1}$  values [17, 18]. We find  $\beta_s$  values close to 1 above 1 K, indicating a homogeneous system, and somewhat decreasing at low temperature, e.g., leading to values 0.7–0.85 at 0.27 K in the 3.2–7.4 T magnetic field range, as shown in Fig. 4(b). Only one point in this figure has  $\beta_s = 0.5$ , corresponding to the obviously inhomogeneous phase mixture at the phase transition point.

## EXPERIMENTAL RESULTS

### NMR spectra

Figure 1 shows the evolution of the  $^{31}\text{P}$ -NMR spectra across the previously mentioned structural phase transition. At 248 K we see two NMR lines corresponding to the *two* phosphorus sites of the structure, as also observed by NMR in the paramagnetic and fully polarized phases of  $\text{Pb}_2\text{VO}(\text{PO}_4)_2$  [11, 19] and in  $\text{SrZnVO}(\text{PO}_4)_2$  [9] vanadates: the P1 site is localized inside the planes of  $\text{V}^{4+}$  spins, it is thus more strongly coupled to them, and

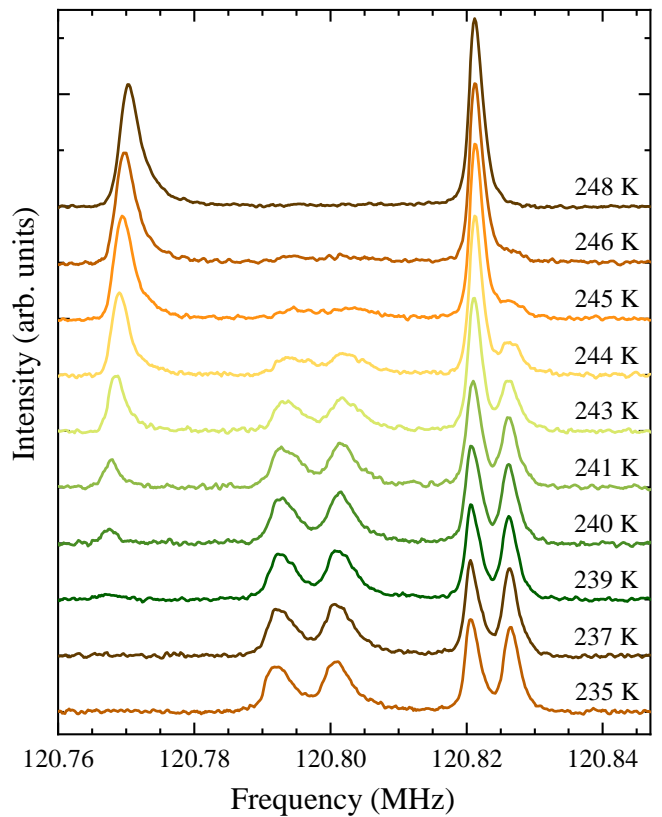


FIG. 1. Temperature dependence of  $^{31}\text{P}$ -NMR spectra of  $\text{BaCdVO}(\text{PO}_4)_2$  in the field of 7 T applied parallel to  $c$  axis, covering the structural phase transition at  $T_s \sim 240 \text{ K}$ .

corresponds to the broader NMR line at lower frequency; the P2 site is localized between these planes, it is less coupled to the spins, and corresponds to the narrower NMR line at higher frequency. Below the structural phase transition appears a modulation in the  $b$ -axis direction which *doubles* the number of *all* crystalline sites [13] (Supplemental Material), creating in particular an alternation of two different  $\text{V}^{4+}$  spin sites (see Fig. 1 in Ref. [14]) as well as an alternation of the two P1a and P1b sites in the planes of spins and the two P2a and P2b sites in between these planes. In the spectra at 235 K and 237 K we see the *four* corresponding NMR lines: there is a low-frequency pair of broader P1a and P1b lines and a high-frequency pair of narrower P2a and P2b lines. Finally, as expected for a first order phase transition, the NMR spectra between 239 K and 246 K present a mixture of the high- and low-temperature spectra, reflecting the mixed phase region.

The magnetic field dependence of low-temperature spectra measured at  $T = 0.27 \text{ K}$  (Fig. 2) presents above  $\mu_0 H_{c1} = 4.05 \text{ T}$  a four-peak structure that is fully analogous to that seen at high temperatures. This is a clear signature that above  $H_{c1}$  the system is *homogeneously* polarized, without any trace of some dipolar magnetic order. A quantitative analysis of the spectra collected

above  $H_{c1}$  was obtained in a rather straightforward four-peak fit, where the slightly asymmetric shape of each NMR line was described by a gaussian-based function that was ad hoc modified by a damped third order term:  $\propto \exp[-(\frac{x-x_c}{w})^2 + b * (\frac{x-x_c}{w})^3 / (1.0 + c * |\frac{x-x_c}{w}|^3)]$ . The asymmetry-defining parameters were optimized on the 5-tesla spectrum to the  $b = 0.30$  and  $c = 0.0075$  values and then kept fixed to ensure the same line asymmetry for all fits. The thus obtained peak positions ( $x_c$ ) are shown in the figure by symbols. They carry local information on the spin polarization, that is magnetization  $M$ : the latter stands in a linear relation with the frequency shift of each line. In practise, the temperature dependence of  $M$  was monitored in two ways: *i*) by following the frequency shift of the lowest-frequency P1a line, because stronger coupling of P1 sites to spins provides best sensitivity and because the P1a line avoids an overlap with the neighboring P1b line, and *ii*) by following the separation between the highest- and the lowest frequency line, i.e., their *relative* frequency shift, which avoids the uncertainty of the magnetic field calibration. In order to better approach the zero-temperature values and thus exclude thermal effects [20], the line positions of these two NMR lines were remeasured at 0.10 K and the magnetization for  $H > H_{c1}$  extracted using both methods is plotted against field in Fig. 3(a). For comparison, the same plot shows the Faraday balance magnetometry data from Ref. [13]. The agreement is very good, proving the previous observation that  $\mu_0 H_{c1}$  corresponds to a transition towards full saturation, and that the magnetization process continues to higher fields.

Below  $H_{c1}$  and at low temperature, a spontaneous AF ordering occurs [13, 16], so that each NMR line is expected to be split in two, where the difference in the coupling strength (the hyperfine coupling tensor) is expected to give much stronger splitting for the P1 lines than for the P2 lines, as was observed in  $\text{Pb}_2\text{VO}(\text{PO}_4)_2$  [11, 19]. In  $\text{BaCdVO}(\text{PO}_4)_2$  (Fig. 2) this creates quite complicated spectra with overlapping lines, where we can reasonably recognize that P1a line is indeed strongly split, P1b is unexpectedly only strongly broadened without visible splitting, while the two P2 lines are weakly split as expected. As regards the absence of AF splitting of the P1b NMR line, this finds a simple explanation in the up-up-down-down stripe type of AF order [16] (see there Fig. 3): P1 phosphorus sites are approximately centred within 4 neighboring  $\text{V}^{4+}$  spins, meaning that one type of P1 sites “sees” either 4 up or 4 down spins while the other type “sees” always 2 up and 2 down spins. It is then obvious that the former sites observe strong AF local field, providing a strong splitting of the P1a NMR line, while for the latter ones the local field approximately cancels out, leading to the absence of splitting of the P1b NMR line.

In order to distinguish the overlapping lines, we have selected the NMR spectrum at 3.9 T that visibly pro-

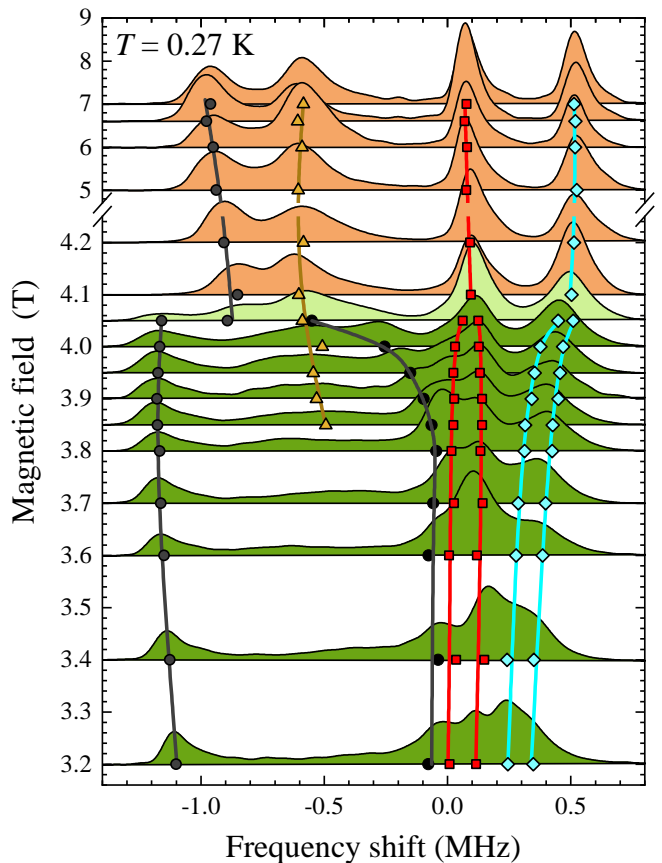


FIG. 2. Magnetic field dependence of the low-temperature (0.27 K)  $^{31}\text{P}$ -NMR spectra, plotted as a function of the frequency shift with respect to the Larmor frequency  $^{31}\gamma\mu_0 H$  ( $^{31}\gamma = 17.236$  MHz/T), in order to reflect the local spin polarization value. Each spectrum is normalized to its integral and offset vertically according to the field value. Symbols are the peak positions obtained by fitting individual spectra, as described in the text. The curves drawn through the symbols are guides for the eye.

vides the best line separation, enabling us to perform a reliable fit to 7 independent line position, and thus fully define all the three line splittings. As the splittings are all proportional to the Néel order parameter (OP) of the AF phase, which is the staggered transverse spin component, their relative size (ratio) should be field independent. We used this additional constraint to stabilize the fits of all the other low-field spectra that are less well resolved: in these fits we fixed the two ratios of the AF line splitting to the values obtained at 3.9 T. Thus obtained line positions are shown in Fig. 2 by symbols, and the corresponding splitting of the P1a line, providing an NMR image of the OP, is presented in Fig. 3(b) and compared with the corresponding information given by neutrons: the structure factor (square root of intensity) of the  $(0, 1/2, 0)$  magnetic Bragg reflection reported in Ref. [14]. One obvious discrepancy between the two data sets is that some residual neutron intensity persists above the transition. That

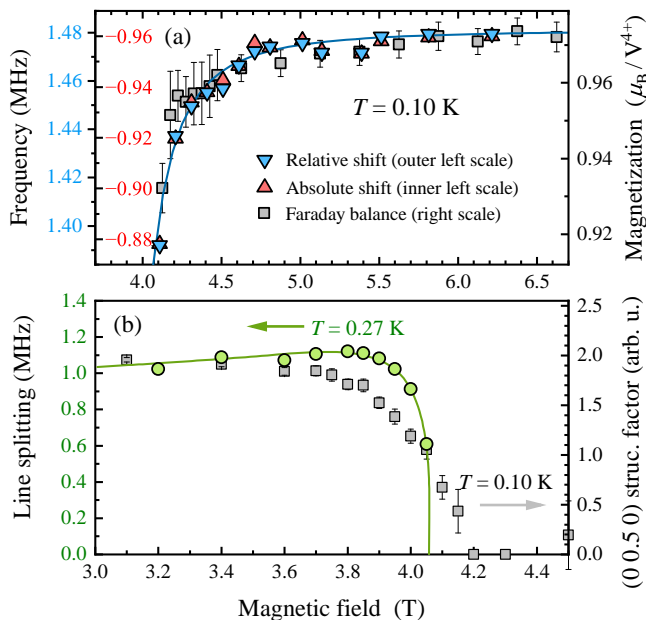


FIG. 3. (a) Field dependence of the sample magnetization above  $H_{c1}$  at 0.10 K, deduced from the relative frequency shift of two NMR lines (down triangles, outer left scale) and from the absolute shift of the lowest-frequency line (up triangles, inner left scale), in comparison to direct Faraday balance magnetometry data (squares, right scale) from Ref [13] and the prediction (solid curve, right scale) given by Eq. (2), see the text. (b) Circles present the field dependence of the magnetic order parameter at 0.27 K, deduced from the line splitting of NMR lines below  $H_{c1}$  (the curve is a guide for the eye). Squares present the structure factor of the magnetic Bragg reflection  $(0, 1/2, 0)$  at 0.10 K, obtained from the neutron data in Ref. [13].

is a known effect due to the finite wave vector and energy resolution of a neutron instrument, which is unable to tell apart between infinitely sharp Bragg peaks due to long range order and broader scattering around the Bragg peak positions due to critical fluctuations. More interesting is that, unlike the neutron measurement, our NMR experiment indicates a non-monotonic behavior of the order parameter. Here, we would observe that both techniques are sensitive to a conceivable rotation of the OP (direction of canting), which is quite possible in the presence of complex DM interactions: NMR line splitting is affected through the angle dependence of the hyperfine coupling constant and neutron intensities through the so-called polarization factor. Nevertheless, the data shown in Fig. 3(b) altogether point rather to a quite flat field dependence of the Néel OP, which is also what has been theoretically predicted for quantum spin-nematic candidates close to the nematic phase, see Fig. 5 in [15].

### $T_1^{-1}$ relaxation rate

To better understand the low-energy spin dynamics below and above saturation, we performed measurements of the  $T_1^{-1}$  relaxation rate vs. field and temperature. The field dependence at two fixed temperatures is shown in Fig. 4(a) on a logarithmic scale. The most obvious features in the  $T_1^{-1}(H)$  plot at  $T = 0.27$  K are the cusps corresponding to the phase transitions at  $H_{c1}$  and at  $\mu_0 H_{c2} \approx 6.50$  T. While the latter appears weak on the logarithmic scale, it still corresponds to a two-fold increase of the relaxation rate, a clear sign of a continuous phase transition. Its position exactly corresponds to the  $H_{c2}$  transition previously detected as a lambda-anomaly in calorimetry experiments [13]. The big  $T_1^{-1}(H)$  peak obviously corresponds to the critical spin fluctuations related to the phase transition at  $H_{c1}$ , and tells us that this transition is essentially of the second order. However, in Fig. 2 we see that the spectrum taken at  $H_{c1}$  corresponds to a *mixture* of the two phases, and we could even measure the two different  $T_1^{-1}$  rates corresponding to each of these two phases [Fig. 4(a)]. Similar behavior was also observed in  $\text{Pb}_2\text{VO}(\text{PO}_4)_2$  [11] and in other quantum spin systems at the phase boundary of the low-temperature AF phase, reflecting weak first-order character of the transition, as predicted for a spin system that presents some magnetoelastic coupling [21, 22].

The observed behavior of the relaxation rate above  $H_{c1}$  is superficially similar to that previously seen in  $\text{SrZnVO}(\text{PO}_4)_2$  [9], however, a quantitative analysis reveals substantial discrepancies. In all cases we consider relaxation via thermal activation across an energy gap that scales proportionately to the single-magnon gap  $\Delta(H) = g\mu_B\mu_0(H - H_c)/k_B$  (here in kelvin units), where  $g = 1.92$  is the  $g$ -factor [12] and  $\mu_B/k_B = 0.67171$  K/T. Furthermore, the log scale of Fig. 4(a) converts an exponential dependence  $\propto e^{-\alpha\Delta/T}$  into its exponent that depends linearly on field, and  $\alpha$  is defined by the magnitude of the slope of the apparent linear dependence. While for a single-magnon condensation in the 3D regime just above the saturation field this slope corresponds to  $\alpha_0 \approx 3$  [9], from Fig. 4(a) we find that the initial value of the slope is very close to 2, which is expected *above* the saturation field of a spin-nematic phase. In more details, fitting the initial slope at 0.27 K in the 4.05–4.3 T range we get  $\alpha = 1.90(9)$ , and at 1.6 K for the 4.05–6.0 T range we get the identical value,  $\alpha = 1.91(2)$ . In order to cover by the fit all the 0.27 K data up to the highest field (excluding the peak centered at  $H_{c2}$ ), we used the *three* activated-terms fit:

$$T_1^{-1}(H) = A(e^{-\alpha_0\Delta/T} + a_1e^{-\Delta/T} + a_xe^{-\alpha_x\Delta/T}), \quad (1)$$

where the second term accounts for the expected presence of the *single-magnon* relaxation and the third term additionally allows for an unexpected spin dynamics showing

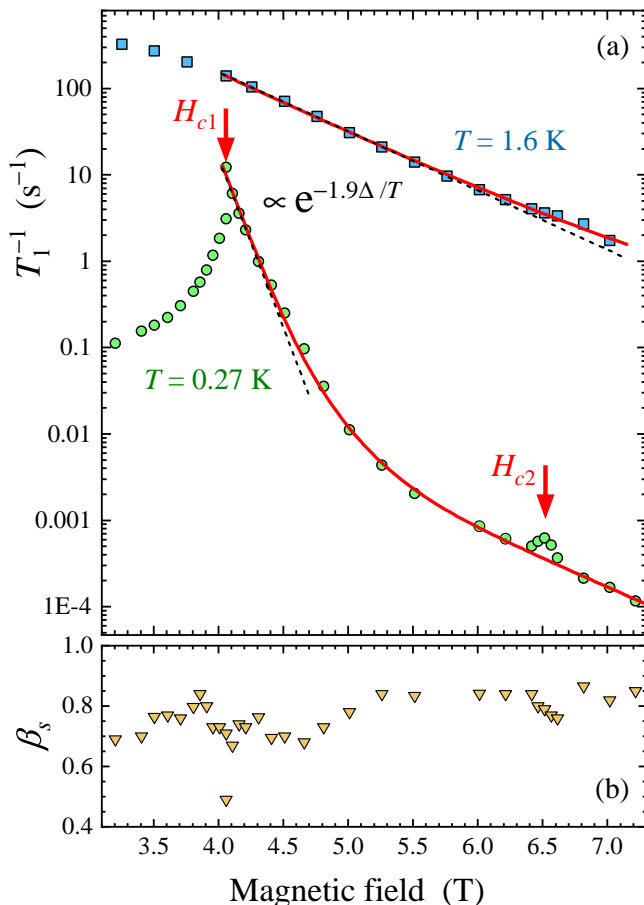


FIG. 4. (a) The  $T_1^{-1}$  relaxation rate measured in  $\text{BaCdVO}(\text{PO}_4)_2$  at 1.6 K (squares) and 0.27 K (circles) as a function of magnetic field applied along the  $c$  axis. Experimental error bars are smaller than the symbol size. Straight dashed lines show activated behaviour with energy gaps that scale with the single-magnon gap  $\Delta(H)$  and red solid curves are the global three-exponential fit given by Eq. (1), as explained in the text. (b) Field dependence of the stretching exponent  $\beta_s$  from the fits to the measured relaxation curves at 0.27 K.

up at high field values (6.0–7.2 T). Using a global, 6-parameter  $[A(T_1), A(T_2), \alpha_0, a_1, a_x, \alpha_x]$  fit over the *both* data sets shown in Fig. 4(a) as a function of  $\Delta(H) \propto H - H_{c1} \geq 0$ , we indeed confirm that  $\alpha_0 = 2.05(4)$  is equal to 2 within its experimental error. Equivalently, fixing  $\alpha_0 = 2$  leads to a nearly indistinguishable fit, which is then preferred because it can be related to the two-magnon spin-nematic fluctuations. In this latter fit we get that the relative size of the single-magnon term amplitude (as compared to the leading two-magnon term) is only  $a_1 = 6.8(7)\%$ , and that the low-temperature high-field term is still much smaller,  $a_x = 0.15(3)\%$ , and has strongly reduced gap  $\alpha_x = 0.32(2)$ .

This analysis suggests the overwhelming dominance of the two-magnon processes. This is quite unusual and very different from what is seen in  $\text{SrZnVO}(\text{PO}_4)_2$ ,

where it is the three- and single-magnon processes, expected for the single-magnon BEC state, that provide the main relaxation mechanisms. Further confirmation for the prevalence of two-magnon relaxation in the high-field phase of  $\text{BaCdVO}(\text{PO}_4)_2$  is found in temperature-dependent measurements at constant fields, shown in Fig. 5. To analyse these data, we recall that, for a gapped system and purely parabolic  $d$ -dimensional magnon dispersion, the preexponential factor of the  $T_1^{-1}$  rate is a powerlaw  $A(T) = A_0 T^\beta$ , where  $\beta = d - 1$ . For the real dispersion relation of magnons in a specific material, the exponent  $\beta$  becomes temperature dependent, reflecting the “effective” dimension of the system, see the Supplemental Material of Ref. [23]. We have thus fitted the  $T_1^{-1}(T)$  using the *same* three-exponential function given by Eq. (1) and having the parameters defined in the previous fit, where the common prefactor is taken to be an ad hoc modified powerlaw  $A(T) = A_0 T^{\beta(T)}$  that allows for a suitable  $\beta(T) = \beta_0 - \beta_1 \log(T/[\text{K}])$  dependence. This provided a remarkably precise *global* fit of the data for all the field values  $\geq H_{c1}$ , covering as much as 1.5 orders of magnitude in temperature and nearly 5 orders of magnitude in  $T_1^{-1}$  for the 5.5 T data in particular. The fit defines three parameters,  $A_0 = 76(1) \text{ s}^{-1}$ ,  $\beta_0 = 1.40(3)$  and  $\beta_1 = 0.82(3)$ , leading to the expected  $\beta(T)$  dependence: at low temperature the system is approaching the 3D regime and  $\beta(0.3 \text{ K}) = 1.8$  is indeed close to the expected  $\beta_{3D} = 2$  value, while the expected 2D regime value  $\beta_{2D} = 1$  is reached at 3.1 K. The validity of the fit at its high temperature end is limited by the validity of the employed  $A(T)$  dependence and the “ $T < \text{gap}$ ” condition for a description as an activated process.

The available low-temperature data show that at 5.5 T there is a continuity of the  $T_1^{-1}(T)$  dependence down to the lowest temperature. This points to the continuity of the phase and the absence of any low-temperature ordering. There is only a crossover into an apparent linear dependence, observed below 0.2 K. Similar crossover seems to be observed below 0.1 K at 3.5 T, where the system is in the AF-ordered phase, so that such behaviour may be associated with the Goldstone mode that is expected to show up at the low-temperature end if the axial symmetry is not broken [24]. However, considering the similarity with the 5.5 T data and the probable presence of the (subdominant) symmetry-breaking anisotropic terms of the Hamiltonian, such an interpretation is questionable. One might rather think of some common low-temperature physics that might be related to sub-leading terms of the system’s Hamiltonian. Finally, inside the AF-ordered phase, for the 3.5 T data in the intermediate temperature range (0.4–0.7 K), we find a strong powerlaw-like behavior, with the power exponent close to 5, as is usually the case in the BEC-type low-temperature phases of quantum antiferromagnets [11, 25–27], reflecting a high-order relaxation process

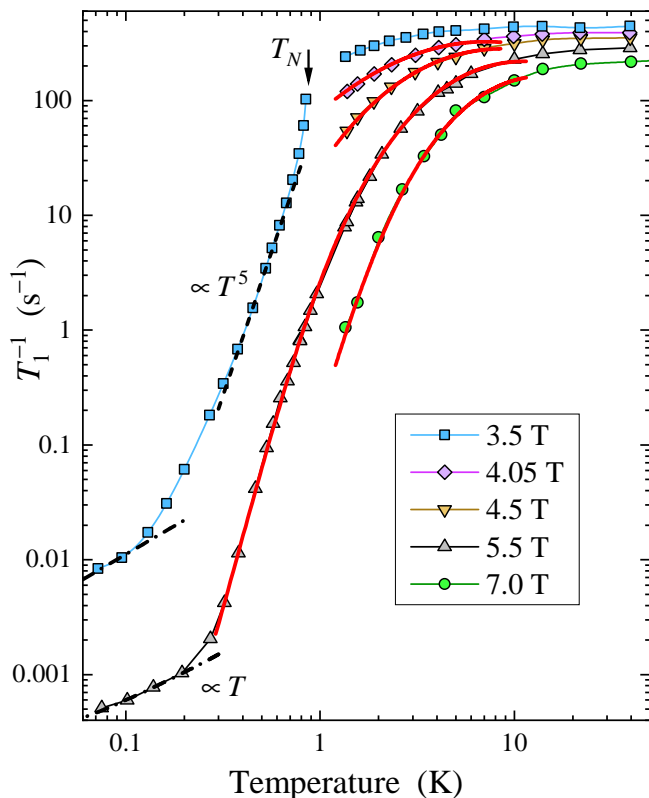


FIG. 5. The  $T_1^{-1}$  relaxation rate measured in  $\text{BaCdVO}(\text{PO}_4)_2$  as a function of temperature at several values of magnetic field applied along the  $c$  axis (symbols). Experimental error bars are smaller than the symbol size. In a wide range above  $H_{c1}$ , the relaxation can be globally fit using the previously defined three-exponential fit [Eq. (1)] where the amplitude is taken to be a modified powerlaw  $A \propto T^{\beta(T)}$ , as explained in the text (red solid curves). At the lowest temperatures,  $T_1^{-1}(T) \propto T$  (dash-dot lines). In the Neel phase below  $H_{c1}$ ,  $T_1^{-1}$  has a characteristic  $\sim T^5$  behavior (dashed line).

[28].

## DISCUSSION AND CONCLUSION

As regards to the phase that appears above  $H_{c1} \approx 4.05$  T in  $\text{BaCdVO}(\text{PO}_4)_2$ , our NMR results provide, in addition to a solid independent validation of the main findings and conjectures of Ref. [13], new microscopic information that is crucial in defining the nature of these phases:

(i) The low-temperature NMR spectra have exactly the same four-peak structure as those in the paramagnetic regime (Fig. 1), and are nearly field independent from  $H_{c1}$  up to the full polarization saturation above 7 T (Fig. 2). This provides clear evidence that the local spin polarization is homogeneous and without any transverse dipolar order, which is indeed one of the necessary (but not sufficient) characteristics of the spin-

nematic phase [29]. The field dependence of the NMR line shift confirms and refines the previously observed field dependence of magnetization: the magnetization at  $H_{c1}$  is slightly (by  $\approx -6\%$ ) reduced as compared to full saturation, and continues to increase in a wide range of fields above  $H_{c1}$  [Fig. 3(a)]. The measurements being carried out at 0.10 K, this dependence is certainly not of thermal origin [20], but it is not necessarily a consequence of some hidden order. It can as well originate from a small anisotropy of the main exchange couplings. For an anisotropy of the  $J_{xx} \neq J_{yy} \neq J_{zz}$  type, this has been discussed in the context of the  $\text{LiCuVO}_4$  compound [29, 30]. In the following paragraph we focus on the terms of the DM type, expected to provide the largest effect in  $\text{BaCdVO}(\text{PO}_4)_2$ . We give a simplest estimate of this effect in the classical approximation and show that the observed field dependence is compatible with this mechanism [Fig. 3(a)]. Finally, we observe that new theoretical predictions for the size of the magnetization variation in the spin-nematic phase [15] speak of a *sizeable* variation, definitely much bigger than the observed 6%. Altogether, the static information is not really favorable to the existence of the spin-nematic phase in  $\text{BaCdVO}(\text{PO}_4)_2$ .

The DM interactions can be rather complex in  $AA'\text{VO}(\text{PO}_4)_2$  structures [10]. To get a ballpark estimate, let us consider a toy model: we take the classical energy of two sublattices coupled by a single DM vector that is normal to the applied field. In the saturated state, DM coupling leads to a small canting of spins by an angle  $\theta$  away from the field direction. This is driven by the gain in the DM energy per spin  $E_{\text{DM}}(\theta) = -DS^2 \sin(2\theta)/2$ . It is stabilized by the corresponding loss of the Zeeman energy per spin  $E_Z(\theta) = -gS\mu_B\mu_0 H \cos\theta$ , reduced by the modification of the exchange energy  $E_J(\theta) = \tilde{J}S^2 \cos(2\theta)/2$ , where  $\tilde{J}$  is some combination of exchange constants that will depend on how the two sublattices become canted. For small canting, the angle dependence of the total energy is quadratic,  $E(\theta) = e_0 - e_1\theta + e_2\theta^2$ , and the equilibrium angle  $\theta_0$  is defined by its minimum,  $\theta_0 = e_1/(2e_2)$ , where  $e_1 = DS^2$  and  $e_2 = gS\mu_B\mu_0 H/2 - \tilde{J}S^2$ . The depolarization  $(1 - \cos\theta_0)$  is then:

$$\frac{\delta M}{M} \approx \frac{1}{2} \left[ \frac{DS}{g\mu_B\mu_0(H - \tilde{H})} \right]^2, \quad (2)$$

where  $g\mu_B\mu_0\tilde{H} = 2\tilde{J}S$ . Since the classical Néel state is the one that minimizes the exchange energy between its two sublattices, we can expect that  $\tilde{H} < H_c$ ,  $H_c$  being the classical saturation field. The latter is equal to the single-magnon instability field, and previously shown to more or less coincide with  $H_{c1}$  in  $\text{BaCdVO}(\text{PO}_4)_2$  [14]. This simplest classical model can indeed reproduce the magnetization data of Fig. 3(a) (solid line) with very reasonable values  $\tilde{H} = 3.75$  T and  $DS^2 = 0.006$  meV. The latter corresponds to 1.6% of the average  $|J_1|$  and is comparable to the crude estimate based on the value of the

spin flop field [13]:  $D/J \sim (H_{\text{SF}}/H_{c1})^2 \sim 1.5\%$ .

(ii) The most important contribution of NMR is certainly the insight in the low-energy spin fluctuations, measured by the  $T_1^{-1}$  relaxation rate. First, the continuity of  $T_1^{-1}(H)$  dependence measured at 0.27 K definitely confirms the continuity of the phase between  $H_{c1}$  and  $H_{c2}$  [Fig. 4(a)]. The peak of  $T_1^{-1}(H)$  centered at  $H_{c2}$  is certainly a signature of some second order phase transition, but the apparent continuity of the data below and above this peak indicates that the nature of the spin fluctuations is probably the same on both sides, suggesting that this might as well be the same phase, whereas the peak is signaling a phase transition appearing at lower temperature. This is strongly reminiscent to the observation of the low-temperature impurity-induced BEC phases in doped  $\text{Ni}(\text{Cl}_{1-x}\text{Br}_x)_2 \cdot 4\text{SC}(\text{NH}_2)_2$  (DTNX) compound [27, 31–33], although in  $\text{BaCdVO}(\text{PO}_4)_2$  it is not clear what might be the source of such impurities. Next, the continuity of the  $T_1^{-1}(T)$  dependence down to 75 mK measured at 5.5 T (Fig. 5) confirms the absence of any phase transition into an ordered state; only a crossover from an essentially activated into a low-temperature linear regime is observed at 0.2–0.3 K. This suggests that above  $H_{c1}$  we see only a nearly fully polarized phase, presenting at very low temperature a crossover into some low-temperature physics, probably related to subdominant terms of the Hamiltonian or/and some defects and/or impurities.

The  $T_1^{-1}$  data and fits shown in Figs. 4(a) and 5 provide clear and quantitatively precise identification of the largely dominant two-magnon relaxation process. Such a relaxation, expected *above* the second critical (= saturation) field of the spin nematic phase, should be regarded as one of the key signatures of this phase. This type of relaxation was already observed above the saturation field of volborthite [34], below which a putative spin-nematic phase was clearly detected [35], but experimental precision of these NMR data was not sufficient to distinguish between the two- and the three-magnon process. In any case, the two-magnon relaxation is *not* expected above the *first* critical field of such a phase, which would be the case if such a phase existed in  $\text{BaCdVO}(\text{PO}_4)_2$  between  $H_{c1}$  and  $H_{c2}$ .

Finally, new theoretical simulations of a spin-nematic phase [15] point to a *very narrow* field range where such a phase is expected, which is clearly not the case for the two critical fields of  $\text{BaCdVO}(\text{PO}_4)_2$ , where  $H_{c2} = 1.60H_{c1}$ . Furthermore, as already pointed out,  $H_{c1}$  coincides with the theoretical prediction for a *single*-magnon instability field [14]. Altogether, all the evidence points to the fact that  $H_{c1}$  is in fact the saturation field of the system, whereas what is observed at  $H_{c2}$  is related to some very low temperature ordered phase of undefined origin and unrelated to the dominant terms of the system's Hamiltonian. The observed two-magnon relaxation process above  $H_{c1}$  then implies that the system is very close to the spin-

nematic instability, so that the corresponding fluctuations dominate the spin dynamics, but the spin-nematic phase is in fact *not* stabilized in  $\text{BaCdVO}(\text{PO}_4)_2$ . This situation appears to be archetypal for other spin-nematic candidate compounds, and our results establish NMR-based criteria to define the true nature of their high-field phases.

We are grateful for the stimulating discussions with Nic Shannon, Tsutomu Momoi and Mike Zhitomirsky. This work was supported, in part, by the Swiss National Science Foundation, Division II.

\* <http://www.neutron.ethz.ch/>

† [mladen.horvatic@lncmi.cnrs.fr](mailto:mladen.horvatic@lncmi.cnrs.fr)

- [1] H. T. Ueda and T. Momoi, Nematic phase and phase separation near saturation field in frustrated ferromagnets, *Phys. Rev. B* **87**, 144417 (2013).
- [2] O. A. Starykh and L. Balents, Excitations and quasi-one-dimensionality in field-induced nematic and spin density wave states, *Phys. Rev. B* **89**, 104407 (2014).
- [3] N. Shannon, T. Momoi, and P. Sindzingre, Nematic order in square lattice frustrated ferromagnets, *Phys. Rev. Lett.* **96**, 027213 (2006).
- [4] H. T. Ueda, Magnetic Phase Diagram Slightly below the Saturation Field in the Stacked  $J_1 - J_2$  Model in the Square Lattice with the  $J_C$  Interlayer Coupling, *J. Phys. Soc. Jpn.* **84**, 023601 (2015).
- [5] R. Nath, A. A. Tsirlin, H. Rosner, and C. Geibel, Magnetic properties of  $\text{BaCdVO}(\text{PO}_4)_2$ : A strongly frustrated spin- $\frac{1}{2}$  square lattice close to the quantum critical regime, *Phys. Rev. B* **78**, 064422 (2008).
- [6] A. A. Tsirlin, B. Schmidt, Y. Skourski, R. Nath, C. Geibel, and H. Rosner, Exploring the spin- $\frac{1}{2}$  frustrated square lattice model with high-field magnetization studies, *Phys. Rev. B* **80**, 132407 (2009).
- [7] A. A. Tsirlin and H. Rosner, Extension of the spin- $\frac{1}{2}$  frustrated square lattice model: The case of layered vanadium phosphates, *Phys. Rev. B* **79**, 214417 (2009).
- [8] F. Landolt, K. Povarov, Z. Yan, S. Gvasaliya, E. Ressouche, S. Raymond, V. O. Garlea, and A. Zheludev, Spin correlations in the frustrated ferro-antiferromagnet  $\text{SrZnVO}(\text{PO}_4)_2$  near saturation, *Phys. Rev. B* **106**, 054410 (2022).
- [9] K. M. Ranjith, F. Landolt, S. Raymond, A. Zheludev, and M. Horvatić, NMR evidence against a spin-nematic nature of the presaturation phase in the frustrated magnet  $\text{SrZnVO}(\text{PO}_4)_2$ , *Phys. Rev. B* **105**, 134429 (2022).
- [10] F. Landolt, Z. Yan, S. Gvasaliya, K. Beauvois, E. Ressouche, J. Xu, and A. Zheludev, Phase diagram and spin waves in the frustrated ferro-antiferromagnet  $\text{SrZnVO}(\text{PO}_4)_2$ , *Phys. Rev. B* **104**, 224435 (2021).
- [11] F. Landolt, S. Bettler, Z. Yan, S. Gvasaliya, A. Zheludev, S. Mishra, I. Sheikin, S. Krämer, M. Horvatić, A. Gazizulina, and O. Prokhnenko, Presaturation phase in the frustrated ferro-antiferromagnet  $\text{Pb}_2\text{VO}(\text{PO}_4)_2$ , *Phys. Rev. B* **102**, 094414 (2020).
- [12] K. Y. Povarov, V. K. Bhartiya, Z. Yan, and A. Zheludev, Thermodynamics of a frustrated quantum magnet on a square lattice, *Phys. Rev. B* **99**, 024413 (2019).

- [13] V. K. Bhartiya, K. Y. Povarov, D. Blosser, S. Betler, Z. Yan, S. Gvasaliya, S. Raymond, E. Ressouche, K. Beauvois, J. Xu, F. Yokaichiya, and A. Zheludev, Pre-saturation phase with no dipolar order in a quantum ferro-antiferromagnet, *Phys. Rev. Research* **1**, 033078 (2019).
- [14] V. K. Bhartiya, S. Hayashida, K. Y. Povarov, Z. Yan, Y. Qiu, S. Raymond, and A. Zheludev, Inelastic neutron scattering determination of the spin Hamiltonian for  $\text{BaCdVO}(\text{PO}_4)_2$ , *Phys. Rev. B* **103**, 144402 (2021).
- [15] S. Jiang, J. Romhányi, S. R. White, M. E. Zhitomirsky, and A. L. Chernyshev, Where is the quantum spin nematic?, *Phys. Rev. Lett.* **130**, 116701 (2023).
- [16] M. Skoulatos, F. Rucker, G. J. Nilsen, A. Bertin, E. Pomjakushina, J. Ollivier, A. Schneidewind, R. Georgii, O. Zaharko, L. Keller, C. Rüegg, C. Pfleiderer, B. Schmidt, N. Shannon, A. Kriele, A. Senyshyn, and A. Smerald, Putative spin-nematic phase in  $\text{BaCdVO}(\text{PO}_4)_2$ , *Phys. Rev. B* **100**, 014405 (2019).
- [17] D. C. Johnston, Stretched exponential relaxation arising from a continuous sum of exponential decays, *Phys. Rev. B* **74**, 184430 (2006).
- [18] V. F. Mitrović, M.-H. Julien, C. de Vaulx, M. Horvatić, C. Berthier, T. Suzuki, and K. Yamada, Similar glassy features in the  $^{139}\text{La}$  NMR response of pure and disordered  $\text{La}_{1.88}\text{Sr}_{0.12}\text{CuO}_4$ , *Phys. Rev. B* **78**, 014504 (2008).
- [19] R. Nath, Y. Furukawa, F. Borsa, E. E. Kaul, M. Baenitz, C. Geibel, and D. C. Johnston, Single-crystal  $^{31}\text{P}$  NMR studies of the frustrated square-lattice compound  $\text{Pb}_2\text{VO}(\text{PO}_4)_2$ , *Phys. Rev. B* **80**, 214430 (2009).
- [20] M. Pregelj, A. Zorko, D. Arčon, M. Klanjšek, O. Zaharko, S. Krämer, M. Horvatić, and A. Prokofiev, Thermal effects versus spin nematicity in a frustrated spin- $\frac{1}{2}$  chain, *Phys. Rev. B* **102**, 081104 (2020).
- [21] R. Dell'Amore, A. Schilling, and K. Krämer,  $U(1)$  symmetry breaking and violated axial symmetry in  $\text{TlCuCl}_3$  and other insulating spin systems, *Phys. Rev. B* **79**, 014438 (2009).
- [22] E. Wulf, D. Hüvonen, R. Schönemann, H. Kühne, T. Herrmannsdörfer, I. Glavatsky, S. Gerischer, K. Kiefer, S. Gvasaliya, and A. Zheludev, Critical exponents and intrinsic broadening of the field-induced transition in  $\text{NiCl}_2 \cdot 4\text{SC}(\text{NH}_2)_2$ , *Phys. Rev. B* **91**, 014406 (2015).
- [23] S. Mukhopadhyay, M. Klanjšek, M. S. Grbić, R. Blinder, H. Mayaffre, C. Berthier, M. Horvatić, M. A. Continentino, A. Paduan-Filho, B. Chiari, and O. Piovesana, Quantum-critical spin dynamics in quasi-one-dimensional antiferromagnets, *Phys. Rev. Lett.* **109**, 177206 (2012).
- [24] T. Giamarchi and A. M. Tsvelik, Coupled ladders in a magnetic field, *Phys. Rev. B* **59**, 11398 (1999).
- [25] H. Mayaffre, M. Horvatić, C. Berthier, M.-H. Julien, P. Ségransan, L. Lévy, and O. Piovesana, NMR Evidence for a “Generalized Spin-Peierls Transition” in the High-Magnetic-Field Phase of the Spin Ladder  $\text{Cu}_2(\text{C}_5\text{H}_{12}\text{N}_2)_2\text{Cl}_4$ , *Phys. Rev. Lett.* **85**, 4795 (2000).
- [26] M. Jeong, H. Mayaffre, C. Berthier, D. Schmidiger, A. Zheludev, and M. Horvatić, Magnetic-order crossover in coupled spin ladders, *Phys. Rev. Lett.* **118**, 167206 (2017).
- [27] A. Orlova, H. Mayaffre, S. Krämer, M. Dupont, S. Capponi, N. Laflorencie, A. Paduan-Filho, and M. Horvatić, Detection of a disorder-induced bose-einstein condensate in a quantum spin material at high magnetic fields, *Phys. Rev. Lett.* **121**, 177202 (2018).
- [28] D. Beeman and P. Pincus, Nuclear spin-lattice relaxation in magnetic insulators, *Phys. Rev.* **166**, 359 (1968).
- [29] A. Orlova, E. L. Green, J. M. Law, D. I. Gorbunov, G. Chanda, S. Krämer, M. Horvatić, R. K. Kremer, J. Wosnitzer, and G. L. J. A. Rikken, Nuclear Magnetic Resonance Signature of the Spin-Nematic Phase in  $\text{LiCuVO}_4$  at High Magnetic Fields, *Phys. Rev. Lett.* **118**, 247201 (2017).
- [30] R. Hagemans, J.-S. Caux, and U. Löw, Gapped anisotropic spin chains in a field, *Phys. Rev. B* **71**, 014437 (2005).
- [31] A. Orlova, R. Blinder, E. Kermarrec, M. Dupont, N. Laflorencie, S. Capponi, H. Mayaffre, C. Berthier, A. Paduan-Filho, and M. Horvatić, Nuclear Magnetic Resonance Reveals Disordered Level-Crossing Physics in the Bose-Glass Regime of the Br-Doped  $\text{Ni}(\text{Cl}_{1-x}\text{Br}_x)_2-4\text{SC}(\text{NH}_2)_2$  Compound at a High Magnetic Field, *Phys. Rev. Lett.* **118**, 067203 (2017).
- [32] M. Dupont, S. Capponi, and N. Laflorencie, Disorder-Induced Revival of the Bose-Einstein Condensation in  $\text{Ni}(\text{Cl}_{1-x}\text{Br}_x)_2-4\text{SC}(\text{NH}_2)_2$  at High Magnetic Fields, *Phys. Rev. Lett.* **118**, 067204 (2017).
- [33] M. Dupont, S. Capponi, M. Horvatić, and N. Laflorencie, Competing Bose-glass physics with disorder-induced Bose-Einstein condensation in the doped  $S = 1$  antiferromagnet  $\text{Ni}(\text{Cl}_{1-x}\text{Br}_x)_2-4\text{SC}(\text{NH}_2)_2$  at high magnetic fields, *Phys. Rev. B* **96**, 024442 (2017).
- [34] M. Yoshida, K. Nawa, H. Ishikawa, M. Takigawa, M. Jeong, S. Krämer, M. Horvatić, C. Berthier, K. Matsui, T. Goto, S. Kimura, T. Sasaki, J. Yamaura, H. Yoshida, Y. Okamoto, and Z. Hiroi, Spin dynamics in the high-field phases of volborthite, *Phys. Rev. B* **96**, 180413 (2017).
- [35] Y. Kohama, H. Ishikawa, A. Matsuo, K. Kindo, N. Shannon, and Z. Hiroi, Possible observation of quantum spin-nematic phase in a frustrated magnet, *Proc. Natl. Acad. Sci. U.S.A.* **116**, 10686 (2019).